

# Properties of Dielectric BaTiO<sub>3</sub> Thin Films Prepared by Spray Pyrolysis

Nickolay Golego, S. A. Studenikin, and Michael Cocivera\*

Guelph-Waterloo Centre for Graduate Work in Chemistry, University of Guelph,  
Guelph, Ontario N1G 2W1, Canada

Received March 10, 1998. Revised Manuscript Received May 15, 1998

Thin-film BaTiO<sub>3</sub> has been prepared for the first time by spray pyrolysis. Both smooth and highly porous films were deposited depending on deposition temperature and rate. As-deposited films contained an unidentified, low-symmetry barium titanate modification. Annealing at 500–900 °C converted the films to the cubic phase, while annealing at 1000 °C produced the tetragonal phase and an increase in the grain size. As-deposited and annealed films were highly dielectric with DC resistivity in the 10<sup>10</sup>–10<sup>12</sup> Ω·cm range. AC resistivity decreased with frequency following a power-law dependence with an exponent of –0.6 to –0.7. Both resistivity and capacitance remained stable at temperatures to 400 °C. The effective dielectric constant (20–25 at 10 kHz) was possibly determined by amorphous grain-boundary region with high density of traps.

## Introduction

Barium titanate, BaTiO<sub>3</sub>, is considered an attractive advanced material. Considerable research has focused on single-crystal and ceramic BaTiO<sub>3</sub>; however, thin films have also found many applications, such as dielectric layers, capacitors,<sup>1,2</sup> waveguides,<sup>3</sup> ferroelectrics, sensors,<sup>4</sup> and luminescent materials.<sup>5</sup> The interest in the thin-film material has increased recently due to the need for high-dielectric-constant materials for ferroelectric RAM and bypass capacitors for VLSI technology. The paraelectric cubic phase of BaTiO<sub>3</sub> is generally preferred for such applications because it has greater temperature stability than the ferroelectric phase and lacks sharp changes in structure and dielectric constant associated with the phase transitions in the latter. In addition, the paraelectric phase is thermodynamically favored for submicrometer polycrystalline BaTiO<sub>3</sub> due to grain-size effect.<sup>6,7</sup>

Much effort has gone into obtaining high-quality dielectric thin-film barium titanate by several methods, including RF sputtering, sol–gel, electrochemical, hydrothermal, and electrohydrothermal methods. In the present paper, an alternative method, spray pyrolysis, is proposed for the growth of thin-film barium titanate. We have successfully employed spray pyrolysis for a number of other thin-film compounds, such as KTiOPO<sub>4</sub>,<sup>8</sup> RbTiOPO<sub>4</sub>,<sup>9</sup> TiO<sub>2</sub>,<sup>10</sup> and ZnO.<sup>11</sup> It was shown

elsewhere,<sup>10</sup> that when a novel titanium precursor with a low decomposition temperature was used, the deposition temperature could be lowered significantly as compared to commonly used titanium chloride pyrolysis. This allows for deposition of BaTiO<sub>3</sub> thin films at low temperature, which is attractive if the processing of the material is to be integrated into the existing silicon technology.

## Experimental Section

The spray pyrolysis setup and the titanium precursor have been reported in detail elsewhere.<sup>8–10</sup> The precursor was titanium peroxohydroxo complex with the formula Ti(O<sub>2</sub>)OH<sup>+</sup> in aqueous nitric acid.<sup>8</sup> It was synthesized by dissolving metallic titanium powder in concentrated aqueous hydrogen peroxide at room temperature and then treating the formed titanium peroxo gel with diluted nitric acid. A repeated nitric acid/hydrogen peroxide treatment was necessary to prepare a concentrated (270–320 mM) stock solution. An aqueous solution of Ba(NO<sub>3</sub>)<sub>2</sub> (0.1 M) was used as a barium precursor. The spray solution concentration, equimolar with respect to barium and titanium, was varied from 6.5 to 75 mM. No solution degradation due to barium titanate precipitation was observed. Several substrates were used: Corning 7059 glass, quartz, indium–tin oxide (ITO)-coated glass, platinum and aluminum sputtered on the 7059 glass. The substrates were cleaned prior to deposition according to an established procedure.<sup>8</sup> The deposition temperature was measured at the substrate. Wet air was used as a carrier gas.

The films were investigated using scanning electron microscopy (SEM) on a Hitachi S-570 microscope equipped with energy-dispersive spectroscopy (EDS) microanalysis system. Data from several spots across the film were taken to monitor possible inhomogeneity. Film thickness and roughness were measured on a Sloan DEKTAK stylus-type recording profilometer as well as from the SEM cross-section images.

Structural analysis of the films on glass or quartz was done using powder X-ray diffraction (XRD) on a Siemens Kristalloflex diffractometer with Cu K $\alpha$  radiation. The resolution in the whole studied  $2\theta$  range, 20–60°, was high enough to resolve the K $\alpha_1$ –K $\alpha_2$  doublet. The  $\alpha_2$  lines were subtracted from the experimental diffraction data. JCPDS standard

- (1) Joshi, P. C.; Desu, S. B. *Thin Solid Films* **1997**, *300*, 289.
- (2) Liu, W. T.; Cochrane, S.; Lakshmikummar, S. T.; Knorr, D. B.; Rymaszewski, E. J.; Borrego, J. M.; Lu, T. M. *IEEE Electron Device Lett.* **1993**, *14*, 320.
- (3) Gill, D. M.; Block, B. A.; Conrad, C. W.; Wessels, B. W.; Ho, S. T. *Appl. Phys. Lett.* **1996**, *69*, 2968.
- (4) Chen, S. N.; Ramakrishnan, E. S.; Grannemann, W. W. *J. Vac. Sci. Technol. A* **1985**, *3*, 678.
- (5) Block, B. A.; Wessels, B. W. *Appl. Phys. Lett.* **1994**, *65*, 25.
- (6) Batra, I. P.; Wurfel, P.; Silverman, B. D. *Phys. Rev. B* **1973**, *8*, 3257.
- (7) Takeuchi, T.; Yoshizawa, K.; Shiota, Y.; Nakamura, O.; Kageyama, H.; Yamabe, T. *J. Mater. Chem.* **1997**, *7*, 969.

**Table 1. Spray Pyrolysis Deposition Conditions for BaTiO<sub>3</sub> Thin Films Shown in the Corresponding Figures**

figure	deposition T (°C)	spray solution concentrn (mM)	carrier flow rate (L/h)	deposition rate <sup>a</sup> (mL/h)
1a,b	400	6.5	34	0.8
2a,b	200	75	34	1.0
2c,d	350	75	42	2.0
2e,f	350	75	42	3.0
3–5	350	75	42	2.5
6–8	400	7.5	37	1.3
9, 10	350	75	42	2.5

<sup>a</sup> Defined as the volume of the spray solution used per unit deposition time.

database and a diffraction pattern simulation software<sup>12</sup> was used for phase identification. UV–vis optical absorption spectra were recorded on a Shimadzu UV-160U double-beam spectrophotometer from 200 to 1100 nm. Substrate absorption was accounted for by running a blank substrate in the reference beam. Some of the films were annealed in a quartz reactor for 2–5 h at temperatures from 500 to 1000 °C in different ambients (argon, hydrogen, air).

Contacts to the films were made using commercial silver paste or indium metal. Aluminum and platinum contacts (100–400 nm thick) were RF-sputtered in argon at 10 mTorr. A mask was used to deposit several circular electrodes 1 mm in diameter. In some cases, conductive ITO or aluminum was used as a back contact. Conductivity measurements were performed on a homemade high-impedance setup in a constant voltage mode using a Hewlett-Packard E3612A voltage source (0–120 V DC) and Keithley 485 autoranging picoammeter (10<sup>-13</sup> A sensitivity). A solid metal Faraday cell was used to reduce electromagnetic interference noise. Carrier mobility and concentration were determined from Hall effect experiments on a homemade apparatus<sup>13,14</sup> in a magnetic field of 0.8 T using Keithley 220 programmable current source (10<sup>-1</sup>–(5 × 10<sup>-13</sup>)A) and Keithley 197 autoranging digital multimeter. In all cases, the contacts were verified to be ohmic by a current–voltage sweep.

Current–voltage characteristics were recorded on a digital recording oscilloscope (Nicolet Instrument Co., model 2090-III A) connected to a computer and a sweep generator-potentiostat assembly. The same oscilloscope connected to a conventional Sawyer–Tower circuit at 60 Hz was used to study the ferroelectric properties of the films in electric fields up to 10<sup>7</sup> V/m. Dielectric parameters of the material were obtained with blocking electrodes from complex impedance measurements using a Solartron 1173 frequency response analyzer with a 1186 interface in the 10 Hz to 1 MHz range in a planar capacitor geometry.

## Results and Discussion

Depending on the deposition rate and substrate temperature, BaTiO<sub>3</sub> thin films were deposited with a variety of morphologies. The deposition conditions of several films are shown in Table 1. Generally, the temperature and deposition rate dependence followed that previously observed and reported in detail for titanium dioxide.<sup>10</sup> No significant influence of substrate nature on properties of the films was observed. Using

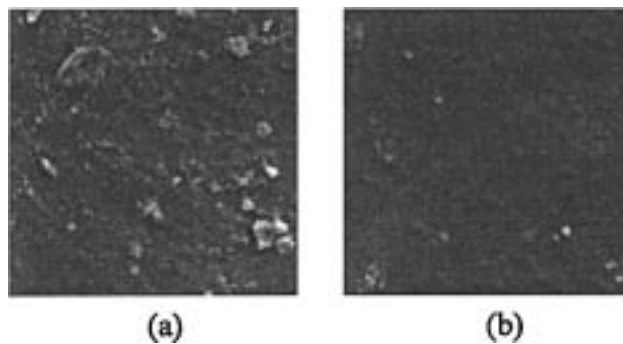


**Figure 1.** SEM images of smooth thin-film BaTiO<sub>3</sub> deposited by spray pyrolysis at low deposition rates, image size 4 × 4 μm (a) as-deposited at 400 °C; (b) annealed in hydrogen at 900 °C for 2 h.

low deposition rates (below 1.5 mL/h from 7.5 to 6.5 mM solutions), smooth, optical-quality films were obtained (Figure 1a). They were thin (under 200 nm) and transparent below the intrinsic absorption edge. A small number of round particles less than 300 nm in diameter were present on the surface. The cross-section images indicated that these particles sat on top of the film and did not penetrate it. It is possible that these particles served as nucleation centers for further film growth. They almost entirely disappeared after annealing at 900 °C (Figure 1b). No cracking or peeling was observed for annealed samples (Figure 1b). A different type of film was deposited from more concentrated solutions (75 mM) at higher deposition rates (2.0–3.0 mL/h). These films were thick (2–5 μm) and opaque, and SEM revealed a high degree of porosity, as seen in Figure 2. Surface roughness increased in comparison to the optical quality films. Low substrate temperature, around 200 °C, gave thick, highly porous films (Figure 2a). Annealing caused crystallization and significant changes in surface morphology (Figure 2b), which may indicate that the as-deposited material was amorphous. Films deposited at higher temperatures (350–400 °C) had a less porous structure (Figure 2c) that was not affected by annealing (Figure 2d). It is interesting that distinctly crystalline films can be prepared at very high deposition rates. In Figure 2e, one can see finely faceted crystallites several micrometers in size. These crystallites did not appear to change their shape upon annealing (Figure 2f), although this treatment caused dramatic changes in the crystalline structure as discussed below. Again, both as-deposited and annealed films were crack-free (Figure 2).

All as-deposited films belonged to a phase that could not be identified using the JCPDS database (Figure 3b). This phase could be a BaO–TiO<sub>2</sub> compound such as barium tetratitanate or other complex titanates. Other likely impurities, such as titanium dioxide, barium carbonate, oxide, or hydroxide, are excluded. None of these compounds was identified from the XRD patterns. In addition, the as-deposited films did not change their mass after prolonged treatment with hot water; hence, no water-soluble compounds were present. The analytical balance that was used in the mass change experiments was capable of recording changes as low as 0.1 mg. The mass of a typical 5 μm-thick film is on the order of 10 mg, assuming an ideal density of 6 g/cm<sup>3</sup>. Several experiments were done to ensure reproducibility, and blank substrate samples were analyzed as

(8) Golego, N.; Cocivera, M. *J. Electrochem. Soc.* **1997**, *144*, 736.

(9) Golego, N.; Cocivera, M. *Thin Solid Films* **1998**, in press.

(10) Golego, N.; Studenikin, S. A.; Cocivera, M. *J. Mater. Res.* **1998**, in press.

(11) Studenikin, S. A.; Golego, N.; Cocivera, M. *J. Appl. Phys.* **1998**, *83*, 2104.

(12) Kraus, W.; Nolze, G. 1996, *Powder Cell 1.8*. ftp://ftp.kfa-juelich.de/iwe/Xtalogy/powdcell/pc18.zip.

(13) Windheim, J.; Renaud, I.; Cocivera, M. *J. Appl. Phys.* **1990**, *67*, 4167.

(14) Windheim, J.; Wynands, H.; Cocivera, M. *J. Electrochem. Soc.* **1991**, *138*, 3435.

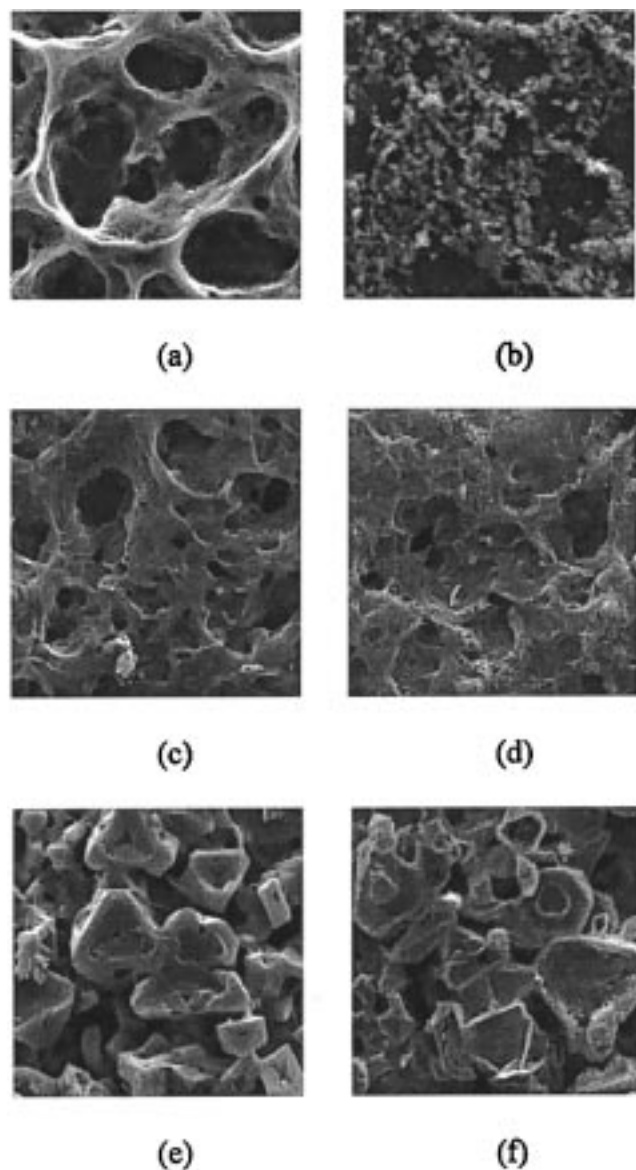


**Figure 2.** SEM images of thin-film BaTiO<sub>3</sub> deposited by spray pyrolysis at high deposition rates (shown in Table 1), image size 20 × 20 μm (a) as-deposited at 200 °C; (b) same, annealed in air at 600 °C; (c) as-deposited at 350 °C; (d) same, annealed in argon at 500 °C; (e) as-deposited at 350 °C; and (f) same, annealed in argon at 500 °C.

well to monitor possible drift of the balance, which was below the detection limit. Moisture pickup was eliminated by drying the films in a drybox and monitoring their mass after taking them out. Therefore, the setup could reproducibly detect mass changes with 1% resolution. No change was observed in all films, although XRD gave low-symmetry peaks of magnitude comparable to that of cubic barium titanate. If this had been an impurity to the latter, its mass should have been a large fraction of the film mass.

The presence of unpyrolyzed precursors is excluded. Although, as has been shown previously,<sup>10,11</sup> spray-pyrolytic deposition at low temperatures can produce films that are not fully pyrolyzed, the deposition temperature in the present work was not less than 200 °C. The titanium precursor has been shown<sup>10</sup> to decompose fully at 120 °C; therefore, it could not have been present in the films. While barium nitrate is a more stable

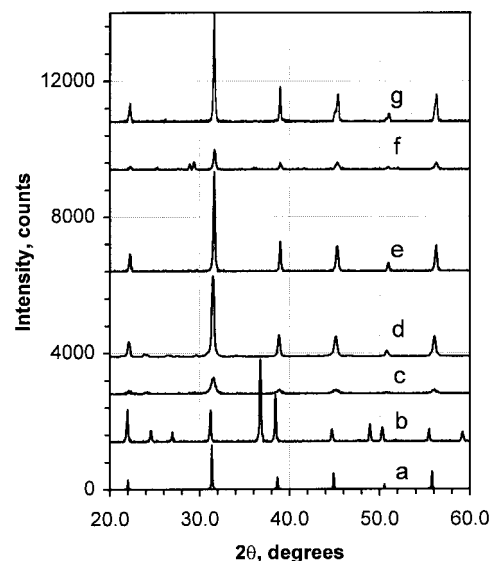


**Figure 3.** XRD pattern of thin-film BaTiO<sub>3</sub> deposited by spray pyrolysis and annealed at different temperatures in different ambients: (a) theoretical cubic; (b) as-deposited at 200 °C; (c) annealed at 500 °C in argon; (d) annealed at 600 °C in air; (e) annealed at 900 °C in air; (f) annealed at 900 °C in hydrogen; (g) annealed at 1000 °C in air.

compound, it was not identified on XRD. Besides, its decomposition during annealing would have changed the mass of the film, but no change was observed.

It is proposed that the as-deposited films contained a low-symmetry barium titanate phase, possibly a complex barium titanate. Indeed, as seen in Figure 3b, the diffraction pattern of the as-deposited films is an extension of that of cubic barium titanate (Figure 3a). SEM investigation provided additional support. As seen in Figure 2e,f, the phase transition from as-deposited phase to cubic barium titanate associated with mild annealing at 500 °C (Figure 3c) did not affect the morphology and crystallite shape of the crystalline films. No change in mass or film thickness was observed also. Because these results are characteristic of a disorder–order transition, the as-deposited film is likely a low-symmetry phase.

Because several samples of ceramic BaTiO<sub>3</sub> that were used as reference had the same XRD pattern as the annealed films, these films were unambiguously identified as cubic barium titanate. Annealing at 500–900 °C did not change the crystalline structure of the material (Figure 3c–e). However, a 1000 °C anneal caused partial phase transformation into the ferroelectric tetragonal barium titanate (Figure 3g) as illustrated more clearly in Figure 4. The XRD peak positions in Figure 4 also indicate that annealing caused a small decrease in crystal lattice parameters. Similar behavior was observed for barium titanate films prepared by sol–gel deposition<sup>15,16</sup> and ion-beam evaporation.<sup>17</sup> It is typically associated with temperature-induced grain growth that removes grain size effects and permits formation of the tetragonal phase. This behavior was confirmed in the present study: a distinctly granular

(15) Nishizawa, H.; Katsube, M. *J. Solid State Chem.* **1997**, *131*, 43.

(16) Takeuchi, T.; Tabuchi, M.; Ado, K.; Honjo, K.; Nakamura, O.; Kageyama, H.; Suyama, Y.; Ohtori, N.; Nagasawa, M. *J. Mater. Sci.* **1997**, *32*, 4053.

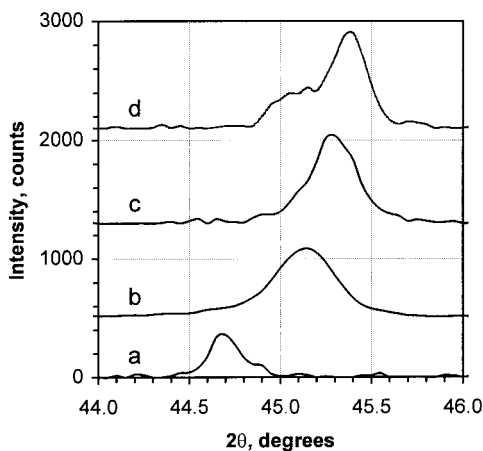


**Figure 4.** Enlarged XRD pattern of thin-film BaTiO<sub>3</sub> deposited by spray pyrolysis and annealed at different temperatures in air: (a) as-deposited at 350 °C; (b) 600 °C; (c) 900 °C; (d) 1000 °C

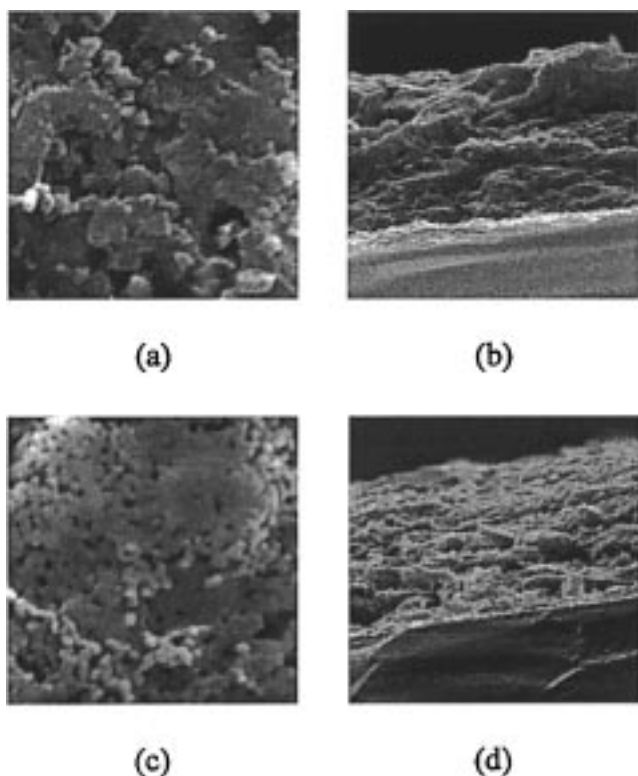


**Figure 5.** SEM images of thin-film BaTiO<sub>3</sub> deposited by spray pyrolysis (a, c, top view, image size 4 × 4 μm, b, d, cross-section, image size 10 × 10 μm): (a, b) as-deposited at 350 °C; (c, d) annealed in air at 1000 °C.

structure is evident in the films annealed at 1000 °C (Figure 5c,d) as compared to as-deposited films (Figure 5a,b). The cross-section images of both films (Figure 5b,d) showed that the films were dense and that the thickness did not change after annealing. The difference in annealing ambients (hydrogen, argon, or air) had no effect on the film morphology. However, annealing at 900 °C in hydrogen caused films to become more conductive and less adhesive to the substrate. In addition, new peaks appeared on the XRD pattern of the hydrogen-annealed films (Figure 3f).

EDS analysis of film composition was complicated by partial overlap of Ba-L with Ti-K, and Ba-M with Ti-L emission lines, respectively, and no precise elemental

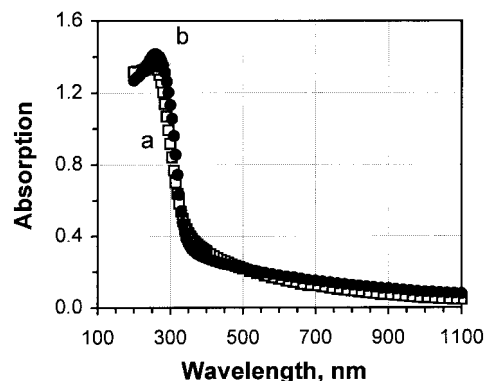


**Figure 6.** Optical absorption spectra of thin-film BaTiO<sub>3</sub> deposited by spray pyrolysis: (a) as-deposited at 400 °C; (b) annealed in air at 1000 °C.

analysis was attempted. Nevertheless, the EDS software provided adequate peak separation and revealed that both as-deposited and annealed BaTiO<sub>3</sub> were homogeneous and same in their composition within the experimental error. The reference samples of BaTiO<sub>3</sub> ceramics were analyzed as well and provided a reliable indication of peak separation quality. One should keep in mind that the identity of the films was additionally confirmed by other analytical methods such as XRD and UV-vis absorption spectroscopy.

UV-vis optical absorption spectra of the films showed that they were transparent below the band gap (Figure 6). Annealing did not change the spectra (Figure 6b vs a), even for hydrogen-annealed films, although the band edge sharpened somewhat for films annealed at high temperatures, 900–1000 °C, probably resulting from film crystallization. Earlier reports of the optical band gap for thin-film BaTiO<sub>3</sub> varied considerably from 2.95<sup>18</sup> to 3.95 eV.<sup>19</sup> Most of these values were calculated from optical absorption spectra using a parabolic conduction band approximation. Although it appears valid for certain well-studied semiconductors, this approach may not be as precise for wide-band gap, perovskite materials such as BaTiO<sub>3</sub>. Calculations of band structure<sup>20,21</sup> indicate that perovskite materials cannot be easily identified as either direct or indirect band gap semiconductors. Large conduction zone anisotropy and nearly flat zone regions that lead to two-dimensional conduction bands<sup>21</sup> may render the parabolic conduction band approximation invalid. Optical band gap values obtained in this way may not be precise and may only be useful for comparison of relative values.

For comparison with previous data, indirect and direct band gap values were calculated from the optical absorption spectra using the above-mentioned model. As shown previously for titanium dioxide,<sup>10</sup> a better fit is obtained by including the dependence of the refractive index on the photon energy. Since these data were not available for the entire energy region studied, the Sellmeier harmonic oscillator model was used to calculate the near-band gap dependence.<sup>22</sup> Values of 3.1–3.2 and 3.7–3.8 eV were obtained for indirect (Figure

(17) Sonogawa, T.; Grigoriu, C.; Masugata, K.; Yatsui, K.; Shimotori, Y.; Furuuchi, S.; Yamamoto H. *Appl. Phys. Lett.* **1996**, *69*, 2193.

(18) Lu, X. M.; Zhu, J. S.; Zhang, W. Y.; Ma, G. Q.; Wang, Y. N. *Thin Solid Films* **1996**, *274*, 165.

(19) Kamalasanan, M. N.; Deepak Kumar, N.; Chandra, S. *J. Appl. Phys.* **1994**, *76*, 4603.

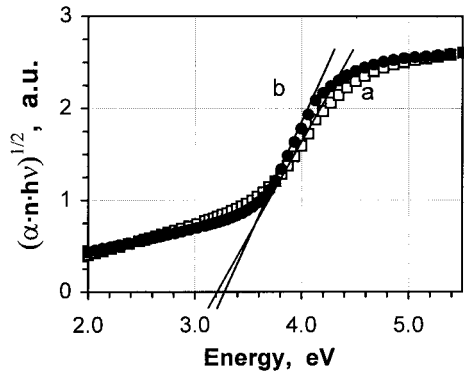


**Figure 7.** Indirect band gap extrapolation for thin-film BaTiO<sub>3</sub> deposited by spray pyrolysis: (a) as-deposited at 400 °C; (b) annealed in air at 1000 °C.

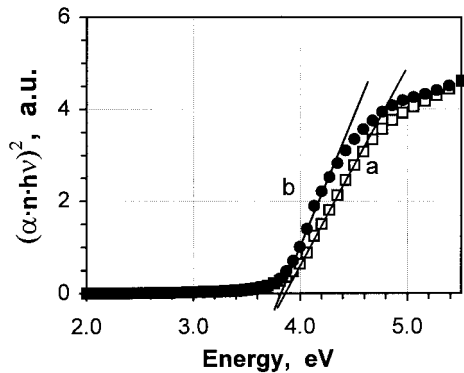


**Figure 8.** Direct band gap extrapolation for thin-film BaTiO<sub>3</sub> deposited by spray pyrolysis: (a) as-deposited at 400 °C; (b) annealed in air at 1000 °C.

7) and direct (Figure 8) band gap extrapolation, respectively. As evident from Figures 7 and 8, annealing did not affect the band gap values. Since the films did not show any appreciable photoconductivity with 365 nm (3.4 eV) light, the direct band gap value seemed to be the preferred one.

The films were very resistive:  $10^{10} \Omega\cdot\text{cm}$  as-deposited and more than  $10^{12} \Omega\cdot\text{cm}$  after annealing. Similar resistivity values were reported previously for films prepared by other techniques.<sup>1,23,24</sup> This large resistivity caused high shot noise in the Hall experiments and dictated the limit of detection of the Hall voltage, which was around 200  $\mu\text{V}$ . Using this limit, the following parameters were estimated: carrier mobility of less than  $0.5 \text{ cm}^2/(\text{V}\cdot\text{s})$  and carrier concentration of more than  $10^{12} \text{ cm}^{-3}$ . The conductivity type was not determined. Up to 400 °C, the temperature dependence of the conductivity was very weak, implying that neither sub-band-gap states nor band-gap transitions were thermally excited at these temperatures. It is evident from these results that the films possessed good dielectric properties.

Complex impedance measurements were performed on Al/BaTiO<sub>3</sub>/Al and ITO/BaTiO<sub>3</sub>/Al planar capacitance

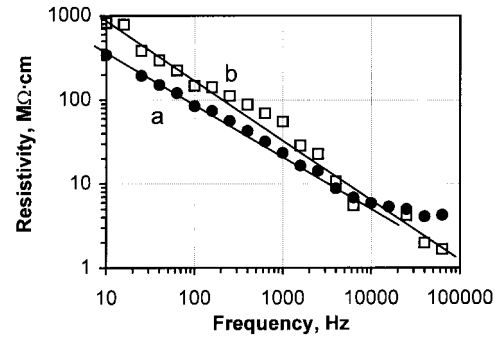


**Figure 9.** Frequency dependence of resistivity for thin-film BaTiO<sub>3</sub> deposited by spray pyrolysis: (a) annealed in argon at 500 °C; (b) as-deposited at 350 °C.

structures and interpreted in terms of a parallel RC circuit. The real part of impedance, or AC resistivity, was frequency-dependent (Figure 9) and could be fitted to a power law dependence  $R \approx \omega^\alpha$ , with  $\alpha$  about  $-0.6$  to  $-0.7$ . A similar decrease in resistivity of the films with the increase in frequency was observed for sol-gel prepared films,<sup>25</sup> and the authors suggested it was due to trapped charge carriers. In polycrystalline BaTiO<sub>3</sub>, these traps may be localized at oxygen-related grain-boundary states<sup>26,27</sup> that were found to dominate electron transport in many polycrystalline oxides such as TiO<sub>2</sub><sup>10</sup> and ZnO.<sup>11</sup> This model is consistent with the increase in resistance at lower frequency because grain boundaries are very thin and, therefore, have a much larger capacitance, which manifests itself in the lower frequency region. As a result, the resistivity of as-deposited films obeyed the power-law dependence in the whole range of the frequency (Figure 9b). On the other hand, the resistance of annealed films leveled off at 10 kHz (Figure 9a), indicating that grain bulk states began to make a contribution at higher frequencies as crystal size increased.

Both resistance and capacitance were stable with temperature. This agrees with the proposed model in which capacitance is determined by temperature-independent grain-boundary capacitance.<sup>26,28,29</sup> The bulk capacitance, which presumably follows the Curie–Weiss law, is expected to show up at a much higher frequency than we were able to attain with our setup. The effective dielectric constant of the films showed a characteristic dispersion with frequency (Figure 10) and was equal to 20–25 at 10 kHz, consistent with the values reported previously.<sup>2,4,17,30</sup> Sawyer–Tower polarization measurements showed paraelectric behavior, as might be expected in view of the structural data, and large leakage currents were observed. Similar behavior for amorphous and polycrystalline BaTiO<sub>3</sub> films<sup>31</sup> led the authors to conclude the amorphous grain-boundary layer had a low dielectric constant and high dielectric losses. Films annealed at 1000 °C had the tetragonal

(20) Wolfram, T.; Kraut, E. A.; Morin, F. J. *Phys. Rev. B* **1973**, *7*, 1677.

(21) Wolfram, T. *Phys. Rev. Lett.* **1972**, *29*, 1383.

(22) Buse, K.; Riehemann, S.; Loheide, S.; Hesse, H.; Mersch, F.; Kratzig, E. *Phys. Stat. Sol. A* **1993**, *135*, K87.

(23) Mohammed, M. S.; Naik, R.; Mantese, J. V.; Schubring, N. W.; Micheli, A. L.; Catalan, A. B. *J. Mater. Res.* **1996**, *11*, 2588.

(24) Kuwabara, M.; Takahashi, S.; Kuroda, T. *Appl. Phys. Lett.* **1993**, *62*, 3372.

(25) Kamalasanan, M. N.; Deepak Kumar, N.; Chandra, S. *J. Appl. Phys.* **1993**, *74*, 5679.

(26) Zhu, W.; Wang, C. C.; Akbar, S. A.; Asiaie, R.; Dutta, P. K.; Alim, M. A. *Jpn. J. Appl. Phys.* **1996**, *35*, 6145.

(27) Russell, J. D.; Leach, C. J. *Eur. Ceram. Soc.* **1996**, *16*, 1035.

(28) Sinclair, D. C.; West, A. R. *J. Appl. Phys.* **1989**, *66*, 3850.

(29) Gerthsen, P.; Hoffmann, B. *Solid-State Electron.* **1973**, *16*, 617.

(30) Cho, C. R.; Kwun, S. I.; Noh, T. W.; Jang, M. S. *Jpn. J. Appl. Phys.* **1997**, *36*, 2196.

(31) Song, M. H.; Lee, Y. H.; Hahn, T. S.; Oh, M. H.; Yoon, K. H. *J. Appl. Phys.* **1996**, *79*, 3744.

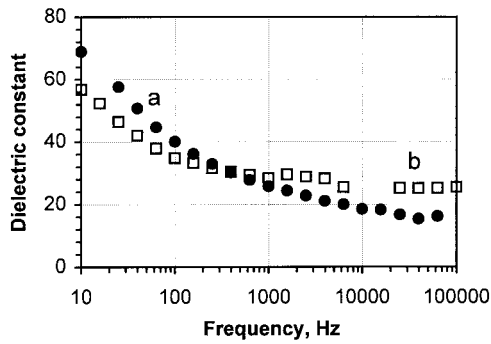


**Figure 10.** Frequency dependence of dielectric constant for thin-film BaTiO<sub>3</sub> deposited by spray pyrolysis: (a) as-deposited at 350 °C; (b) annealed in argon at 500 °C.

structure suitable for ferroelectric behavior. Unfortunately, this behavior could not be studied because the high-temperature destroyed the back-contact.

### Conclusions

Stoichiometric thin-film BaTiO<sub>3</sub> has been prepared for the first time by spray pyrolysis. Either closely packed

or highly porous films could be deposited by regulating the deposition temperature and rate. As-deposited films contained an unidentified, low-symmetry barium titanate phase. Annealing at 500–900 °C converted the films to the cubic phase, while annealing at 1000 °C caused formation of the tetragonal phase and a corresponding increase in the grain size. As-deposited and annealed films were dielectric with DC resistivity in the 10<sup>10</sup>–10<sup>12</sup> Ω·cm range. The AC resistivity decreased with increased frequency and followed a power-law dependence that may be due to grain-boundary traps. Both resistivity and capacitance remained stable at temperatures up to 400 °C. The effective dielectric constant was 20–25 at 10 kHz.

**Acknowledgment.** The authors wish to thank Taras Kolodyazhny (Department of Chemistry, University of Guelph) for the reference samples of barium titanate ceramics. This work was supported in part by a grant to M.C. from the Natural Sciences and Engineering Research Council of Canada.

CM980153+